applied sciences

MDPI

Article

Design of Mode-Locked Fibre Laser with Non-Linear Power and Spectrum Width Transfer Functions with a Power Threshold

Ziyi Xie [1], Junsong Peng [1,2], Mariia Sorokina [3,*] and Heping Zeng [1,4]

[1] State Key Laboratory of Precision Spectroscopy, East China Normal University, Shanghai 200062, China
[2] Collaborative Innovation Center of Extreme Optics, Shanxi University, Taiyuan 030006, China
[3] Aston Institute of Photonic Technologies, Aston University, Birmingham B4 7ET, UK
[4] Chongqing Institute of East China Normal University, Chongqing 401120, China
* Correspondence: m.sorokina@aston.ac.uk

Abstract: There is a growing demand for higher computational speed and energy efficiency of machine learning approaches and, in particular, neural networks. Optical implementation of neural networks can address this challenge. Compared to other neuromorphic platforms, fibre-based technologies can unlock a wide bandwidth window and offer flexibility in dimensionality and complexity. Moreover, fibre represents a well-studied, low-cost and low-loss material, widely used for signal processing and transmission. At the same time, mode-locked fibre lasers offer flexibility and control, while the mode-locking effect can be crucial for unlocking ultra-short timescales and providing ultra-fast processing. Here, we propose a mode-locked fibre laser with a non-linear power threshold in both power and spectrum. The advantage of the proposed system is a spectrum width two-branch function dependent on the input signal power. The effect is caused by a transition between two operating regimes and is governed by the input signal power. The proposed design enables receiving a non-linear transfer function in amplitude with a power threshold as an optical analogue of biological neurons with the additional advantage of a non-linear two-branch transfer function in spectrum width. The latter property is similar to the frequency-varied response dependent on stimulus properties in biological neurons. Thus, our work opens new avenues in research into novel types of artificial neurons with a frequency spectrum width variable response and, consequently, spiking neural networks and neural-rate-based coding with potential applications in optical communications and networks with flexible bandwidth, such as 5G and emerging 6G.

Keywords: optical signal processing; optical neurons; mode-locked fibre lasers

Citation: Xie, Z.; Peng, J.; Sorokina, M.; Zeng, H. Design of Mode-Locked Fibre Laser with Non-Linear Power and Spectrum Width Transfer Functions with a Power Threshold. *Appl. Sci.* **2022**, *12*, 10318. https://doi.org/10.3390/app122010318

Academic Editors: Angelina Totovic and Nikolaos Passalis

Received: 10 April 2022
Accepted: 10 October 2022
Published: 13 October 2022

1. Introduction

There is enormous pressure to increase the speed of processing of an ever-growing volume of information. Developments in machine learning and artificial intelligence create opportunities for a variety of applications for big data technologies, including the Internet of Things and future communications, such as 6G. Neural networks have become one of the leading processing tools, offering a broad range of potential applications and opening up new frontiers.

At the same time, there has been a surge in the development of optical platforms for the realisation of neural networks. In particular, neuromorphic photonics [1–3] pave the way for the fast and energy-efficient realisation of neural networks. Neuromorphic processing and neural networks have a wide range of practical applications in physics, engineering, medicine and other fields, by enabling the processing of various types of signals. There is a growing interest in this area due to novel designs, new hardware implementations, and wide potential application. In particular, recurrent neural networks (RNNs) offer new areas of application ranging from image analysis and classification, speech recognition and

language translation, to advanced research and industry-oriented tasks, such as inverse imaging problems or high-speed communications. Recently, RNNs have been applied in optical communications for non-linear signal distortion compensation [4–6] and non-linearity mitigation for advanced high-order modulation formats [7–9].

While RNNs enable the solution of complex tasks, the complexity of RNNs themselves increases the amount of time required for training and processing. This presents a computational challenge and requires novel computational approaches. Thus, there is a demand for novel electronic and optical hardware platforms to address speed and energy requirements for successful implementation of RNNs. An optical neuron is a key component of such technologies, from the seminal Fitzhugh–Nagumo neuron [10,11] with its electronic realisation in the 1960s and the silicon neuron designed in the 1990s [12], to a silicon analogue of the eye's retina [13] and the Neurogrid network simulating one million neurons [14]. Among different underlying platforms, there are also the advanced silica-wafer-based SpiNNaker and BrainScaleS computing platforms of the Human Brain Project [15], while a 294-fold acceleration against a conventional computer was demonstrated in [16] using silicon photonic weight banks. At the same time, there have been developments in semiconductor RNNs with optical delayed feedback [17] and fibre-based RNNs with gigabyte-per-second speed [18]. Such architectures boast a large number of neurons and intrinsic layers.

An echo state network (ESN) [19] is a type of reservoir computing (RC) [20] approach to the design of RNNs, which reduces training complexity as only output weights are required to be trained. The system can be realized by randomly connected non-linear nodes, which mimic neurons. Moreover, it has been demonstrated that only one non-linear node is required to realise RNNs as time- [21] or frequency-multiplexing [22] can be used to create virtual neurons. Such architectures have already been demonstrated to have practical applications, including in high-speed signal processing, in particular, in optical communications [23–27]. The all-optical implementation of ESN enables high-speed signal processing and can provide the basis for a new generation of high-speed computing hardware [17,28] and address ever-growing demands on signal-processing speed.

Optical neurons are often based on lasers, as it is a mature technology with a broad range of applications and enables control and flexibility in the design. Recently, semiconductor vertical-cavity surface-emitting laser (VCSEL) [29,30] and graphene-based [31] laser neurons have been developed. Optical demonstration of ESN with GHz bandwidth was based on a semiconductor laser [17] for applications in optical networks and communications for amplitude-modulated-signal processing [24]. Higher bandwidth enables higher signal processing speed; moreover, current developments in optical communications and 5/6G employ ultra-wideband signals [32].

However, a fundamental limitation on optical RNN speed is imposed by the underlying material and is related to the relaxation time of the media. Fibre as a processing medium offers a tens-of-THz-order bandwidth window. Fibre-based ESN analogue (FESNA) [25] was the first demonstration of THz bandwidth neuromorphic signal processing. Moreover, fibre, in particular, multi-mode fibre, unlocks multiple degrees of freedom enabling multi-dimensional signal processing [25,33], which is crucial for the solution of complex problems where multiple dimensions need to be processed simultaneously. Moreover, fibre-based NN architecture can be straightforwardly adapted to fibre-based optical communication networks and fibre-based optical-signal-processing methods, which present a mature and well-developed technology. For example, fibre-based optical Fourier transform incorporated into FESNA has enabled the first multi-channel neuromorphic signal processor [22].

Current developments in signal transmission and communications, such as 5G standards, focus on ultrawideband and flexible bandwidth signals [34–36]. Emerging 6G networks are envisioned to merge intelligent processing within the optical communication network [37]; it is, therefore, a requirement for future neuromorphic processing technology to support such flexible bandwidth signal architectures.

Fibre mode-locking is a key to ultra-fast signal-processing as it enables processing over extremely short timescales. Moreover, it paves the way for controlling spectral properties, creating new opportunities in the development of spiking neural networks, which are of major practical importance. Fibre mode-locked laser represents a well-studied technology with ubiquitous dynamics [38,39] and numerous techniques have been developed to augment and assess its capabilities [40,41].

Furthermore, as biological neurons are known to exhibit complex frequency-varied responses to different types of stimulus (for example, the spike frequency adaptation effect [42,43]), which play an essential role in neuronal processing and adaptation, future artificial optical neurons will need to encompass such effects in their design.

In this work, we lay the foundation for such technology by proposing the first photonic system, which exhibits a spiking non-linear response in both power and spectral width governed by a power threshold. Here, we demonstrate the first design of a mode-locked fibre laser with non-linear operating regimes in both power and spectrum width. We show that the proposed laser system exhibits a non-linear power-dependent response with a threshold. We unveil the transition between two operating regimes where the signal experiences a change of attenuation coefficients in the power transfer function and the two-branch transfer function in spectrum width. These features are very important for developing a novel type of optical neuromorphic technology with variable bandwidth capability that can address optical communication system requirements and can unlock the ultra-high-speed neuromorphic processing of ultrashort pulses.

The unique advantage of the proposed system is a non-linear spectral signal re-shaping dependent on signal power with a clear transition gap between the two stages. Since the transition is governed by a power threshold, the system can be used for spectrum coding as a novel type of neural coding. The presented fibre mode-locked laser system is simple and flexible and can be used in a wide range of applications, including in photonics and medicine, such as self-tuning lasers [44,45] and smart sensors [46], as well as optical communications [47,48] and in 5G and 6G networks [22,49].

2. Design

Here, we use a mode-locked fibre laser configuration, which performs non-linear signal processing while the input signal is generated by a seed laser. A seed laser is used here as the most general type of excitation (signal) generator, which represents an input excitation. Given the broad range of applications of neural networks, this setup enables mimicking of signals excited by various physical, engineering or biological systems. Moreover, an unmodulated input enables mapping of the output response to receive a transfer function characteristic of the designed processor. The experimental setup is illustrated in Figure 1. The seed laser (left) is a fibre ring cavity laser in which a 1.25-m-long erbium-doped fibre constitutes the gain medium, pumped by a laser diode operating at 980 nm through a wavelength-division multiplexer. An intracavity programmable spectral shaper (Finisar WaveShaper) is used to adjust the net-cavity dispersion and the central wavelength of the pulses. The frequency of the generated pulses from the seed laser is 18.53 MHz and is constant throughout the experiment. The pump power is fixed to 250 mW. The gain medium is fully relaxed between the input pulses. The mode-locked laser operation is obtained using an effective saturable absorber based on a non-linear polarizaton rotation (NPR) [50] effect realized by three waveplates and a polarizer. The output of the laser after amplification is an input to the processing laser (right) with a similar laser configuration. A variable optical attenuator (VOA) is used to control the energy of the input pulses, without modifying other pulse parameters, such as the pulse duration and the spectral width. The proposed configuration enables changing of the properties of the input excitation, while the processing laser is used to generate a neural response.

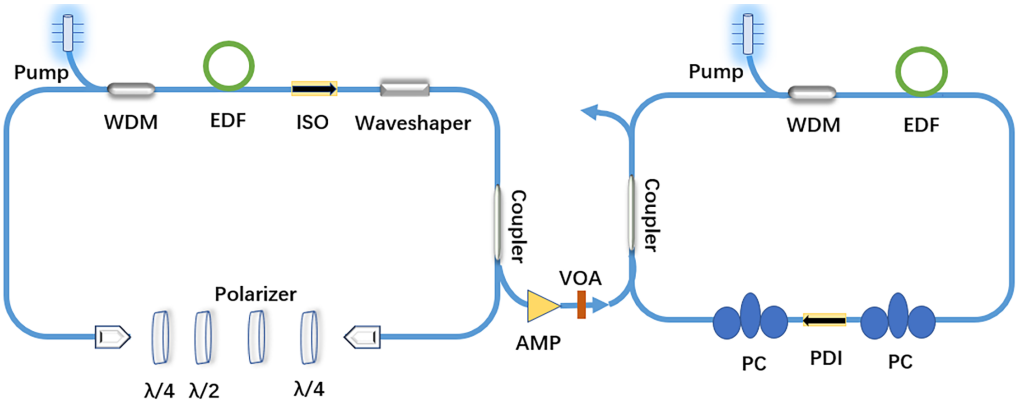

Figure 1. The experimental setup. WDM: wavelength-division multiplexer; EDF: erbium-doped fibre; ISO: isolator; AMP: amplifier; VOA: variable optical attenuator; PDI: polarisation-dependent isolator; PC: polarization controller.

3. Results and Discussion

Figure 2a depicts the initial spectrum of the seed (left) and the processing (right) lasers, respectively. As can be seen, due to anomalous dispersion, the spectrum of the right laser shows Kelly sidebands, which arise from interference between solitons and dispersive waves. In contrast, the pulse spectrum from the left laser has no Kelly sidebands as a result of nearly zero dispersion. When the pulses from the seed (left) laser are input to the processing (right) laser, the output pulses show evolving non-linear dynamics (see Figure 2b). Initially, when the input power is low, the pulse spectrum in the right laser does not change; however, when the input power increases to a threshold (around 125 μW), the Kelly sidebands disappear and the spectrum resembles that of the input pulses. As the input power increases further, the input pulse dominates and the spectrum follows the shape of the input pulse. Thus, the response of the processing laser has a non-linear threshold dependent on an input signal power. An additional advantage of the proposed processor is the controlling of the spectral dynamics by the input signal power.

Figure 3a shows the output power of the laser (right) as the input power from the left laser is varied by VOA. There is an inflection point between 120 and 125 μW. It can be seen that the transfer function on the output power in the vicinity of the inflexion point experiences stationary-like behaviour (the output power does not change significantly in the vicinity of the infection point) with a corresponding drop in the transfer function slope (see Figure 3b. With further increase in the input power, the output power continues to grow and the slope returns to the previous value. This results in a gap in the transfer function compared to the original trend (see the dashed red line in Figure 3a). The drop in power is constant (as shown by the constant slope in the transfer function) after the inflexion point and is caused by the transition into a different lasing regime, resulting in a jump from one branch of a transfer function to another. This behaviour is unique to the proposed system and is accompanied by a two-branch spectrum transfer function (see Figure 4a, which is also a unique advantage of the proposed design.

Therefore, two operating regimes can be distinguished:

(i) below the threshold—the output signal follows the eigen-mode excitation characteristic of the processing laser inherent properties;
(ii) above the threshold—the output signal follows the input signal excitation.

These regimes have different properties, both in the power dynamics characterized by the changes in the amplification/attenuation parameter (variation of the slope in Figure 3b), and in the spectral properties of the signals (see Figures 2 and 4).

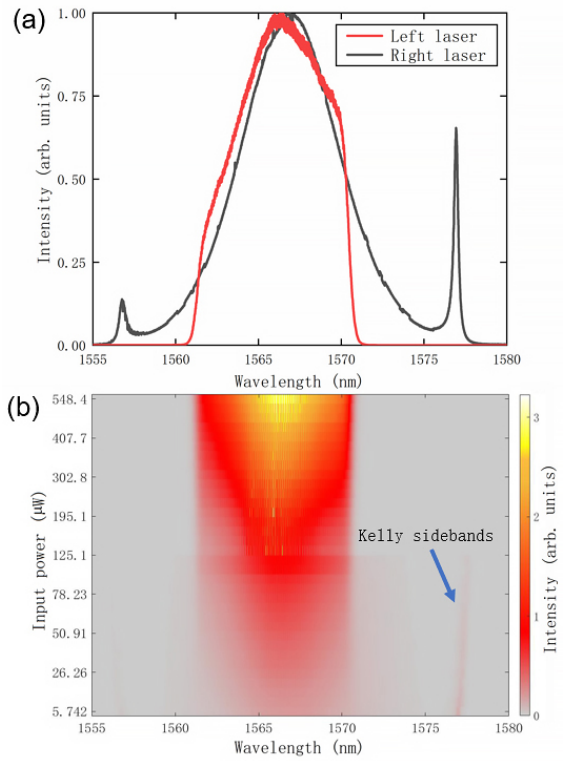

Figure 2. (**a**) The spectrum of the left laser (red) and the spectrum of the right laser when no signal is input to it—self-excitation mode (black); (**b**) the spectra evolution of the right laser when the input signal from the left laser is varied.

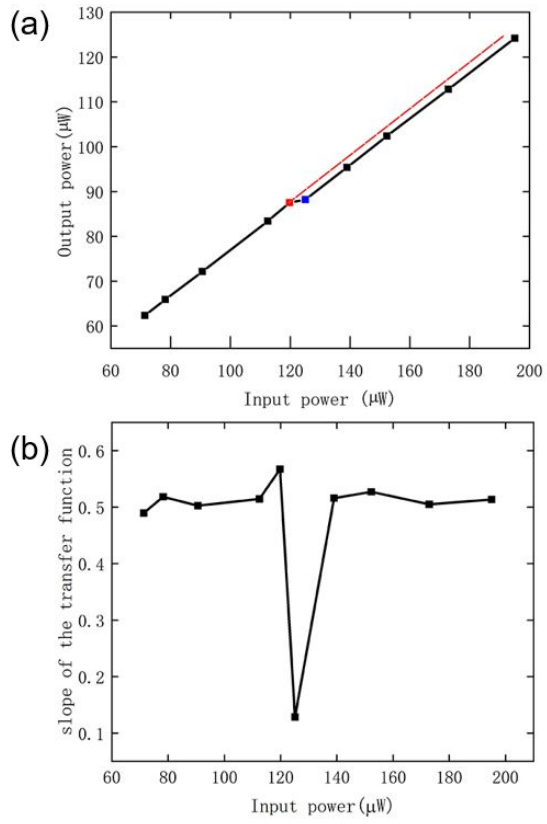

Figure 3. (**a**) Power transfer function: the output power of the laser (right) when the input power of the seed (left) laser is varied by the VOA; (**b**) the slope variation as a function of input power.

The threshold optical power is defined by the properties of the eigen signal generated in the processing laser, in particular, its power. The non-linear dynamics inside the cavity of the processing laser induce signal–signal interactions between the input signal being transformed and the eigen signal being generated inside the cavity. Thus, the threshold power is defined by the parameters of the processing laser, the pumping power as well as the gain medium. Overall, the physics of the process present a new research direction for analytical treatment, as well as improved understanding of the signal–signal dynamic processes inside the cavity, in particular, for the design of new generating and processing regimes in lasers.

The transfer function is identical when increasing or decreasing the input power; it is below the conversion power value at which the mode-locking is destroyed (this value is defined by the cavity parameters of the processing laser; here it is 120 mW).

The proposed technology has a characteristic spiking response with a power threshold and exhibits non-linear behaviour dependent on the input signal power, mimicking biological neurons.

The mode-locking effect in fibre lasers is known to enable processing over ultra-short timescales. As the first demonstration of the laser design, we used an Er-doped fibre as a gain medium for illustration purposes as it is one of the most accessible, low cost and well-studied doped-fibre types, thus achieving an ms-order response time (see Figure 4a). Depending on the relaxation time of the gain medium, it is possible to achieve higher processing speeds targeting ultra-fast processing, which can also benefit from the fibre-based Echo state network architecture (FESNA) [22,25,26], potentially enabling THz-bandwidth processing.

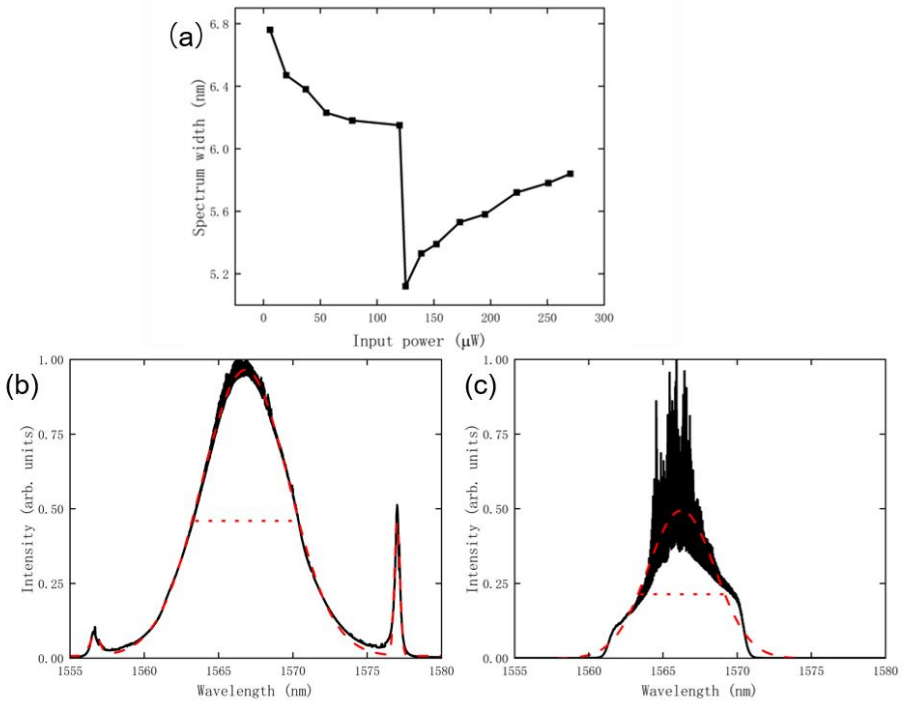

Figure 4. (**a**) The spectrum width of the output signal as the input signal power generated by the seed (left) laser is varied by the VOA; (**b**) the spectrum before the threshold at 5.742 μW input power (here the red dotted line represents Gaussian fitting) with the spectral width 6.83 nm; (**c**) the spectrum after the threshold at 139 μW input power and the corresponding spectral width 5.33 nm.

Moreover, the system offers an additional advantage of non-linear spectral re-shaping dependent on the input signal power similar to biological neurons, which may generate spikes with a frequency dependent on the input excitation. Here the spectral width of the output pulse has a distinct two-branch non-linear response dependent on the input power

(see Figure 4a). The two-branch dependency of the spectrum on the input power is due to the transition between two operating regimes, as explained above, namely:

(i) below the threshold - the non-linearity is small and the output signal spectrum width equals that of the *eigen-signal*, i.e., the signal when the (right) laser operates without the input signal; (ii) above the threshold - for larger non-linearity, the input signal becomes dominant and the output spectrum width equals the width of the *input signal* spectrum.

The distinct gap in the spectrum width in Figure 4a is due to the rapid switch between two regimes. The spectrum is captured via a Yokogawa optical spectrum analyzer (AQ6370D) and calculated at a 3dB pulse width using Gaussian fitting. The spectrum can be compared before the threshold plotted in Figure 4b at 5.742 μW input power (here, the red dotted line represents Gaussian fitting) with the corresponding spectral width 6.83 nm and the spectrum after the threshold plotted in Figure 4c with 139 μW input power and the corresponding spectral width 5.33 nm. The results plotted here are for the 20 mW pump power of the processing laser. With further increase in the pump power the general trends in the amplitude transfer function and the value of the threshold remain the same, while the spectrum width transfer function becomes more step-like and the drop value increases drastically. However, increase in the pump value above 50 mW leads to a multi-pulsing regime. In this work, we focus on single-pulsing only—the emergence of complex dynamics in a multi-pulsing regime will be the subject of further work.

Thus, the proposed technology can lead to a new type of neural coding. In particular, depending on the input power, the spectrum width can be modulated with clearly defined power-dependent regimes with a threshold. Thus, information can be encoded in the spectrum width. This is similar to rate coding. However, rate coding is based on the firing rate, while here, the spectral width of the individual spikes is encoded. Therefore, we refer to this type of coding as spectrum coding. This is a unique advantage of the proposed technology, which is caused by incorporating mode-locking effects in the technology.

Moreover, this is the first optical system that has amplitude-dependent non-linear properties in both amplitude and spectrum width governed by a power-dependent threshold. The design encompasses non-linear processing with power-threshold and spectral re-shaping, paving the way for a novel type of optical neuron with variable bandwidth adapted to the requirements of emerging 6G networks.

4. Conclusions

We propose the first photonic technology based on a mode-locked fibre laser with non-linear properties in both power and spectrum width controlled by a power threshold. Both properties are induced by the mode-locking effect. We distinguish two operating regimes dependent on input signal power with a distinct power threshold, below and above which the output signal follows the spectral shape of a self-excited eigen-signal and an input signal, respectively. The spectral power-dependent re-shaping with a threshold is a unique advantage of the proposed setup and, together with the non-linear power transfer function, paves the way for a new type of optical neuron with two-dimensional non-linearity in power and frequency, similar to biological neurons, which exhibit a frequency-adaptable response depending on the type of input stimulus. Thus, this work opens new directions in the study of artificial neurons with spectrum frequency-adaptable non-linear responses in multiple dimensions, stimulating the development of novel types of neural spectrum coding and neural networks with variable bandwidth for applications in optical communications and networks, 5G and emerging 6G communications.

Author Contributions: Conceptualization, M.S.; investigation, Z.X., J.P. and M.S.; supervision, J.P., M.S. and H.Z.; writing—review and editing, M.S. All authors have read and agreed to the published version of the manuscript.

Funding: Royal Academy of Engineering (RF/201718/17154).

Institutional Review Board Statement: Not applicable.

Informed Consent Statement: Not applicable.

Data Availability Statement: Data underlying the results presented in this paper are not publicly available at this time but may be obtained from the authors upon reasonable request.

Conflicts of Interest: The authors declare no conflict of interest.

References

1. Prucnal, P.R.; Shastri, B.J. *Neuromorphic Photonics*; CRC Press: Boca Raton, FL, USA, 2016.
2. Lugnan, A.; Katumba, A.; Laporte, F.; Freiberger, M.; Sackesyn, S.; Ma, C.; Gooskens, E.; Dambre, J.; Bienstman, P. Photonic neuromorphic information processing and reservoir computing. *APL Photonics* **2020**, *5*, 020901. [CrossRef]
3. Shastri, B.J.; Tait, A.N.; Ferreira, de Lima, T.; Pernice, W.H.P.; Bhaskaran, H.; Wright, C.D.; Prucnal, P.R. Photonics for artificial intelligence and neuromorphic computing. *Nat. Photonics* **2021**, *15*, 102–114. [CrossRef]
4. Jarajreh, M.A.; Giacoumidis, E.; Aldaya, I.; Le, S.T.; Tsokanos, A.; Ghassemlooy, Z.; Doran, N.J. Artificial neural network nonlinear equalizer for coherent optical OFDM. *IEEE Photon. Technol. Lett.* **2015**, *27*, 387–390. [CrossRef]
5. Giacoumidis, E.; Le, S.T.; Ghanbarisabagh, M.; McCarthy, M.; Aldaya, I.; Mhatli, S.; Jarajreh, M.A.; Haigh, P.A.; Doran, N.J.; Ellis, A.D.; et al. Fiber nonlinearity-induced penalty reduction in CO-OFDM by ANN-based nonlinear equalization. *Opt. Lett.* **2015**, *P40*, 5113–5116. [CrossRef]
6. Sorokina, M.; Sygletos, S.; Turitsyn, S. Sparse identification for nonlinear optical communication systems: SINO method. *Opt. Express* **2016**, *24*, 30433–30443. [CrossRef]
7. Hager, C.; Pfister, H.D. Nonlinear Interference Mitigation via Deep Neural Networks. In Proceedings of the Optical Fiber Communication Conference, San Diego, CA, USA, 11–15 March 2018; p. W3A.4 .
8. Shen, T.S.R.; Lau, A.P.T. Fiber nonlinearity compensation using extreme learning machine for DSP-based coherent communication systems. In Proceedings of the 16th Opto-Electronics and Communications Conference, Kaohsiung, Taiwan, 4–8 July 2011; pp. 816–817.
9. Owaki, S.; Nakamura, M. Equalization of optical nonlinear waveform distortion using neural-network based digital signal processing. In Proceedings of the 2016 21st OptoElectronics and Communications Conference (OECC) Held Jointly with 2016 International Conference on Photonics in Switching (PS), Niigata, Japan, 3–7 July 2016; p. WA2-40.
10. FitzHugh, R. Impulses and physiological states in theoretical models of nerve membrane. *Biophys. J.* **1961**. *1*, 445–466. [CrossRef]
11. Nagumo, J.; Arimoto, S.; Yoshizawa, S. An active pulse transmission line simulating nerve axon. *Proc. IRE* **1962**, *50*, 2061–2070. [CrossRef]
12. Mahowald, M.; Douglas, R. A silicon neuron. *Nature* **1991**, *354*, 515–518. [CrossRef]
13. Eliasmith, C.; Stewart, T.C.; Choo, X.; Bekolay, T.; DeWolf, T.; Tang, Y.; Rasmussen, D. A Large-Scale Model of the Functioning Brain. *Science* **2012**, *338*, 1202–1205. [CrossRef]
14. Engel, T.A.; Steinmetz, N.A.; Gieselmann, M.A.; Thiele, A.; Moore, T.; Boahen, K. Selective modulation of cortical state during spatial attention. *Science* **2016**, *354*, 1140–1144. [CrossRef]
15. Calimera, A.; Macii, E.; Poncino, M. The Human Brain Project and neuromorphic computing. *Funct. Neurol.* **2013**, *28*, 191–196.
16. Tait, A.N.; Lima, T.F.; Zhou, E.; Wu, A.X.; Nahmias, M.A.; Shastri, B.J.; Prucnal, P.R. Neuromorphic photonic networks using silicon photonic weight banks. *Sci. Rep.* **2017**, *7*, 7430. [CrossRef]
17. Bueno, J.; Brunner, D.; Soriano, M.C.; Fischer, I. Conditions for reservoir computing performance using semiconductor lasers with delayed optical feedback. *Opt. Express* **2017**, *25*, 2401–2412. [CrossRef]
18. Cohen, E.; Malka, D.; Shemer, A.; Shahmoon, A.; Zalevsky, Z.; London, M. Neural networks within multi-core optic fibers. *Sci. Rep.* **2016**, *6*, 29080. [CrossRef]
19. Lukosevicius, M.; Jaeger, H. Reservoir Computing Approaches to Recurrent Neural Network Training. *Comput. Sci. Rev.* **2009**, *3*, 127–149. [CrossRef]
20. Schrauwen, B.; Verstraeten, D.; Campenhout, J. An overview of reservoir computing: Theory, applications, and implementations. In Proceedings of the European Symposium on Artificial Neural Networks ESANN, Bruges, Belgium, 25–27 April 2007; pp. 471–482.
21. Appeltant, L.; Soriano, M.C.; Van der Sande, G.; Danckaert, J.; Massar, S.; Dambre, J.; Schrauwen, B.; Mirasso, C.R.; Fischer, I. Information processing using a single dynamical node as complex system. *Nat. Commun.* **2011**, *2*, 468. [CrossRef]
22. Sorokina, M. Multi-channel optical neuromorphic processor for frequency-multiplexed signals. *J. Phys. Photonics* **2021**, *3*, 014002. [CrossRef]
23. Bauduin, M.; Massar, S.; Horlin, F. Non-linear satellite channel equalization based on a low complexity echo state network. In Proceedings of the 2016 Annual Conference on Information Science and Systems, Princeton, NJ, USA, 16–18 March 2016; pp. 99–104.
24. Argyris, A.; Bueno, J.; Fischer, I. Photonic machine learning implementation for signal recovery in optical communications. *Sci. Rep.* **2018**, *8*, 8487. [CrossRef]
25. Sorokina, M.; Sergeyev, S.; Turitsyn, S. Fiber echo state network analogue for high-bandwidth dual-quadrature signal processing. *Opt. Express* **2019**, *27*, 2387–2395. [CrossRef]

26. Sorokina, M. Dispersion-managed fiber echo state network analogue with high (including THz) bandwidth. *J. Lightwave Technol.* **2020**, *38*, 3209–3213. [CrossRef]
27. Sackesyn, S.; Ma, C.; Dambre, J.; Bienstman P. Experimental realization of integrated photonic reservoir computing for nonlinear fiber distortion compensation. *Opt. Express* **2021**, *29*, 30991–30997. [CrossRef] [PubMed]
28. Vandoorne, K.; Dambre, J.; Verstraeten, D.; Schrauwent, B.; Bienstman, P. Parallel reservoir computing using optical amplifiers. *IEEE Trans. Neural Netw.* **2011**, *22*, 1469–1481. [CrossRef] [PubMed]
29. Hejda, M.; Robertson, J.; Bueno, J.; Hurtado, A. Spike-based information encoding in vertical cavity surface emitting lasers for neuromorphic photonic systems. *J. Phys. Photonics* **2020**, *2*, 044001. [CrossRef]
30. Heuser, T.; Pflüger, M.; Fischer, I.; Lott, J.A.; Brunner, D.; Reitzenstein, S. Developing a photonic hardware platform for brain-inspired computing based on 5 × 5 VCSEL arrays. *J. Phys. Photonics* **2020**, *2*, 044002. [CrossRef]
31. Shastri, B.J.; Nahmias, M.A.; Tait, A.N.; Rodriguez, A.W.; Wu, B.; Prucnal, P.R. Spike processing with a graphene excitable laser. *Sci. Rep.* **2016**, *6*, 19126. [CrossRef] [PubMed]
32. Ferrari, A.; Napoli, A.; Costa, N.; Fischer, J.K.; Pedro, J.; Forysiak, W.; Richter, A.; Pincemin, E.; Curri, V. Multi-Band Optical Systems to Enable Ultra-High Speed Transmissions. In Proceedings of the European Conference on Lasers and Electro-Optics, Munich, Germany, 23–27 June 2019; p. ci23.
33. Sorokina, M. Multidimensional fiber echo state network analogue. *J. Phys. Photonics* **2020**, *2*, 044006. [CrossRef]
34. Schaich, F.; Wild, T. Waveform contenders for 5G—OFDM vs. FBMC vs. UFMC. In Proceedings of the 6th International Symposium on Communications, Control and Signal Processing (ISCCSP), Athens, Greece, 21–23 May 2014.
35. Christodoulopoulos, K.; Tomkos, I.; Varvarigos, E.A. Elastic bandwidth allocation in flexible OFDM-based optical networks. *J. Light. Technol.* **2011**, *29*, 1354–1366. [CrossRef]
36. The Mobile Broadband Standard Partnership Project. Available online: https://www.3gpp.org/ (accessed on 5 October 2022).
37. Tomkos, I.; Klonidis, D.; Pikasis, E.; Theodoridis, S. Toward the 6G Network Era: Opportunities and Challenges. *IEEE IT Prof.* **2020**, *22*, 32–38.
38. Lecaplain, C.; Grelu, P.; Soto-Crespo, J.; Akhmediev, N. Dissipative rogue waves generated by chaotic pulse bunching in a mode-locked laser. *Phys. Rev. Lett.* **2012**, *108*, 233901. [CrossRef]
39. Peng, J.; Zeng, H. Soliton collision induced explosions in a mode-locked fibre laser. *Commun. Phys.* **2019**, *2*, 34. [CrossRef]
40. Li, B.; Yu, Y.; Wei, X.; Xu, Y.; Tsia, K.K.; Wong, K.K. Real-time observation of round-trip resolved spectral dynamics in a stabilized fs fiber laser. *Opt. Exp.* **2017**, *25*, 8751–8759. [CrossRef]
41. Peng, J.; Sorokina, M.; Sugavanam, S.; Tarasov, N.; Churkin, D.V.; Turitsyn, S.K.; Zeng, H. Real-time observation of dissipative soliton formation in nonlinear polarization rotation modelocked fibre lasers. *Commun. Phys.* **2018**, *1*, 20. [CrossRef]
42. Benda, J.; Herz, A.V.M. A Universal Model for Spike-Frequency Adaptation. *Neural Comput.* **2003**, *15*, 2523–2564. [CrossRef]
43. Izhikevich, E.M. *Dynamical Systems in Neuroscience: The Geometry of Excitability and Bursting*; MIT Press: Cambridge, MA, USA, 2005.
44. Kutz, J.N.; Fu, X.; Brunton, S. Self-tuning fiber lasers: Machine learning applied to optical systems. In Proceedings of the Advanced Photonics Conference, Barcelona, Spain, 27–31 July 2014; p. NTu4A.7 .
45. Baumeister, T.; Brunton, S.L.; Kutz, N.J. Deep learning and model predictive control for self-tuning mode-locked lasers. *J. Opt. Soc. Am. B* **2018**, *35*, 617–626. [CrossRef]
46. Ling, Q.; Gu, Z.; Gao, K. Smart design of a long-period fiber grating refractive index sensor based on dual-peak resonance near the phase-matching turning point. *Appl. Opt.* **2018**, 57, 2693–2697. [CrossRef]
47. Ellis, A.D.; McCarthy, M.E.; Al Khateeb, M.A.Z.; Sorokina, M.; Doran, N.J. Performance limits in optical communications due to fiber nonlinearity. *Adv. Opt. Photon.* **2017**, *9*, 429–503. [CrossRef]
48. Da Ros, F.; Ranzini, S.M.; Dischler, R.; Cem, A.; Aref, V.; Bülow, H.; Zibar, D. Machine-learning-based equalization for short-reach transmission: neural networks and reservoir computing. In Proceedings of the Metro and Data Center Optical Networks and Short-Reach Links IV, Online, 6–12 March 2021; p. 1171205.
49. Luo, F.L.; Zhang, C. *Signal Processing for 5G: Algorithms and Implementations*; Wiley-IEEE Press: Chichester, UK, 2016.
50. Hofer, M.; Ober, M.H.; Haberl, F.; Fermann, M.E. Characterization of ultrashort pulse formation in passively mode-locked fiber lasers. *IEEE J. Quantum Electron.* **1992**, *28*, 720. [CrossRef]